Sādhanā Vol. 27, Part 4, August 2002, pp. 467–484. © Printed in India

Application of size effect to compressive strength of concrete members

JIN-KEUN KIM[1] and SEONG-TAE YI[2]*

[1]Department of Civil & Environmental Engineering, Korea Advanced Institute of Science & Technology, 373-1, Kusong-dong, Yusong-gu, Daejon-si, 305-701, Korea
[2]Department of Civil Engineering, Korea Power Engineering Company Inc., 360-9, Mabuk-ri, Guseong-eup, Yongin-si, Gyeonggi-do, 449-713, Korea
e-mail: kimjinkeun@kaist.ac.kr; yist@kopec.co.kr

Abstract. It is important to consider the effect of size when estimating the ultimate strength of a concrete member under various loading conditions. Well known as the size effect, the strength of a member tends to decrease when its size increases. Therefore, in view of recent increased interest in the size effect of concrete this research focuses on the size effect of two main classes of compressive strength of concrete: pure axial compressive strength and flexural compressive strength.

First, fracture mechanics type size effect on the compressive strength of cylindrical concrete specimens was studied, with the diameter, and the height/diameter ratio considered as the main parameters. Theoretical and statistical analyses were conducted, and a size effect equation was proposed to predict the compressive strength specimens. The proposed equation showed good agreement with the existing test results for concrete cylinders.

Second, the size, length, and depth variations of a flexural compressive member have been studied experimentally. A series of C-shaped specimens subjected to axial compressive load and bending moment were tested. The shape of specimens and the test procedures used were similar to those by Hognestad and others. The test results are curve-fitted using Levenberg–Marquardt's least squares method (LSM) to obtain parameters for the modified size effect law (MSEL) by Kim and co workers. The results of the analysis show that the effect of specimen size, length, and depth on ultimate strength is significant. Finally, more general parameters for MSEL are suggested.

Keywords. Size effect; specimen size; cylindrical specimen; C-shaped specimen; axial compressive strength; flexural compressive strength.

1. Introduction

It is a well known fact that there is an effect of size differences in nominal strength of specimens made with quasibrittle materials such as concrete, rock, ice, ceramic, and composite materials

*For correspondence

(Bažant 1984; Bažant *et al* 1991; Bažant & Xi 1991). More specifically, the nominal strength of laboratory size specimens differ from that of larger structural members used in construction of real structures. The difference in the nominal strength is a direct consequence of energy release into a finite-size fracture process zone (damaged localized zone). In the early 1980's, it became clear that the size effect on the nominal strength of quasibrittle materials failing after large stable crack growth is caused principally by energy release (Bažant & Xi 1991) and cannot be explained by Weibull-type statistics of random micro-defects. Ever since, the problem of size effect has received increasing attention (Bažant *et al* 1991; Bažant & Xi 1991; Bažant & Chen 1997). Description of such a size effect requires energy analysis of fracture mechanics type.

Most concrete structural members experience combined loading conditions composed of compression, tension, moment, and shear. Especially, in the case of reinforced concrete members, the fundamental idea of concrete resisting compressive stress and steel resisting tensile stress is the basic foundation of reinforced concrete structural design. Fracture mechanics-based formulation of size effect theory has not been studied rigorously for compression loaded members.

Gonnerman (1925) experimentally showed that the ratio of the compressive failure stress to the compressive strength decreases as the specimen size increases. This phenomenon of reduction in strength dependent on specimen size is called the "reduction phenomenon". Due to the fracture mechanics-based derivation of size effect law, however, earlier researchers have focused more on pure tension and shear loading conditions rather than compressive loading condition. Only recently, studies (Cotterell 1972; Bažant & Xiang 1994; Jenq & Shah 1991; Bažant & Xiang 1997) on compressive loading based size effect became a focus of interest among researchers.

Currently, researchers in the field accept the conclusion that the failure of concrete loaded in tension is caused by strain localization resulting in a finite size fracture process zone (FPZ). In the last few years, many researchers (Hillerborg 1988, Bažant 1989; Rokugo & Koyanagi 1992; Vonk 1992; Van Mier 1992; Bažant 1993b) have started to realize that the strain localization also occurs for concrete specimens loaded in compression. Unlike failure caused by pure tension loading which usually takes place in a relatively narrow localized zone, compressive loading failure occurs within a larger damage zone. The compressive failure shows a similar failure mechanism as tensile failure. In both cases, the failure is caused by the distributed splitting cracks in the direction of member length as the lateral deformation increases during the failure progression. However, the compressive failure mechanism is more complex than tensile failure mechanism. Size effect of compressive failure is not as distinct as in tensile failure, because the formation of microcracks in compressive failure is distributed in a wider region than in tensile failure.

Presently, most design codes for concrete structures do not consider the effect of size. Since quasibrittle materials fail by formation of cracks, size effect has to be implemented. In compressive failure of quasibrittle materials, the size effect is quite apparent. Though the behaviour of compressive failure has been studied extensively, the failure mechanism and its size effect have been insufficiently studied when compared to tensile failure mechanism. However, endeavouring studies by some researchers have continuously expanded knowledge in the field (Bažant 1987; Bažant 1993a; Bažant & Xiang 1997). Experimental data for proper analyses of size effect is correctly lacking however. From the few available experimental data, it is apparent that compressive strength decreases as specimen sizes increase.

The focus of this study is to further develop and clarify compressive size effect in quasibrittle materials. Compressive strength of concrete can be mainly classified into two main classes:

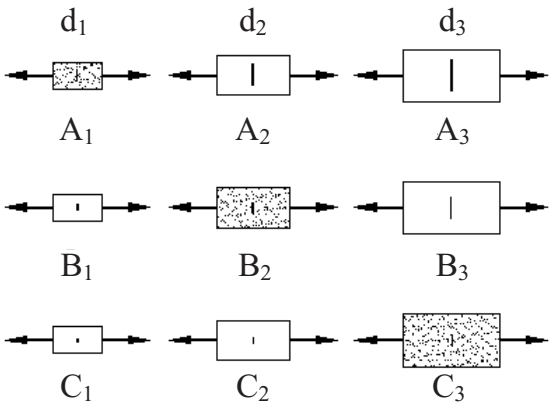

Figure 1. Illustration of similar specimen series (horizontal) and dissimilar specimen series (diagonal).

pure axial compressive strength and flexural compressive strength. In the case of pure axial compressive strength of concrete, there are abundant experimental data from past studies to derive its size effect characteristic. However, for the case of flexural compressive strength of concrete, experiments must be performed to obtain sufficient data to study its size effect.

2. Theoretical investigation on size effect

In materials such as metals the size effect is not observed in the absence of initial cracks. The failure of such materials occurs not due to cracking, but due to considerable plastic deformation. It is well-known, however, that concrete shows size effect even when it has no initial crack.

Bažant (1984) derived size effect law (SEL) from dimensional analysis and similitude arguments for geometrically similar structures of different sizes with initial crack considering the energy balance at crack propagation in concrete.

$$\sigma_N = P_u/bd = Bf_t'/[1 + (d/\lambda_o d_a)]^{1/2}, \tag{1}$$

where, σ_N is nominal strength, P_u is maximum load, b is thickness of specimen, d is characteristic dimension, f_t' is direct tensile strength of concrete cylinder, d_a is maximum aggregate size, and B and λ_o are empirical constants.

In fact, concrete specimens without initial crack are not considered to have the same relative crack length, but rather the same initial lengths for cracks such as pre-existing interfacial bond cracks. It is thus necessary to take into account the influence of a/d on the size effect for concrete specimens without initial cracks. This can be done by taking the parameter λ_o in Bažant's equation as a function of a/d, implying a smaller value of λ_o as the specimen size increases. As a consequence, Bažant's size effect law can be modified in the form of the following equation by introducing a monotonically decreasing function $f(a/d)$,

$$\sigma_N = Bf_t'/[\{1 + (d/f(a/d)d_a\}]^{1/2}. \tag{2}$$

To explain the concept of (2), specimen series are considered as shown in figure 1. These are three geometrically similar specimen series denoted by A, B, and C, with different crack length/specimen depth ratios a/d. The size effect for each series follows Bažant's size effect law, as the function $f(a/d)$ for each series has some constant value. However, the diagonal

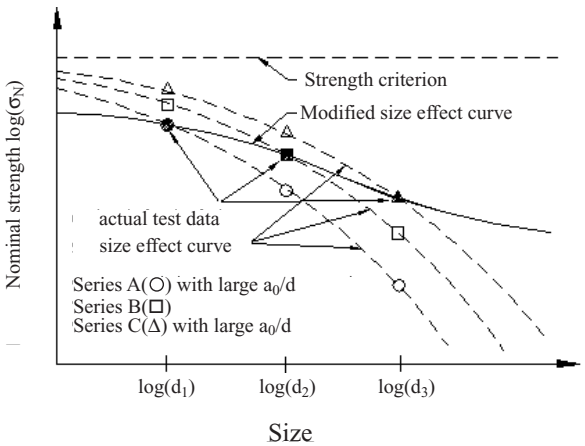

Figure 2. Trend of modified size effect in concrete structures of different a/d ratio.

specimen series consisting of the specimens denoted by A_1, B_2, and C_3 may show the size effect in accordance with (2), as these have the same crack length but different a/d ratios.

The size effect of real concrete specimens without initial cracks can be evaluated from such diagonal specimen series with initial cracks dissimilar to the specimen sizes. In other words, if specimens A_1, B_2, and C_3 have the same maximum aggregate size, the same initial crack length can be assumed, as the crack can be taken as pre-existing, such as an interfacial bond crack. On the other hand, the initial crack length a_o is clearly distinguished from the advanced crack length at failure a. However, there seems to be no difficulty in discussing the geometrical similarity of the specimen series in figure 1, as the two crack lengths a_o and a can both be expressed analogously as a function of the maximum aggregate size.

Figure 2 shows the trend of modified size effect for the diagonal specimen series. According to Bažant's size effect law, nominal strengths at failure for each row specimen series should behave as shown by dotted lines in figure 2. The value of $f(a/d)$ corresponding to λ_o decreases gradually from series A (large a/d) to series C (small a/d). Thus, the real size effect for the specimens A_1, B_2 and C_3 can be predicted with the modified size effect curve of (2), which provides a smooth transition from series A to series C showing a gradual trend in size effect due to the decreasing value of $f(a/d)$. Unfortunately, it is very difficult to derive the function $f(a/d)$ exactly. The crack length at failure a is also not easily measured experimentally. Thus, a new empirical formula is suggested for the purpose of regression analyses within some practical range of sizes. There is little difference in strength reduction trends.

Thereafter, introducing the size independent strength $\sigma_o(= \alpha f_t')$, Kim & Eo (1990) and Kim *et al* (1989) proposed an MSEL (modified SEL), which was also proposed by Bažant (1987), Bažant (1993a), and Bažant & Xiang (1997) in a different approach, given by

$$\sigma_N = \left\{ B f_t' / [1 + (d/\lambda_o d_a)]^{1/2} \right\} + \alpha f_t', \tag{3}$$

where α is an empirical constant less than unity.

The value of $\lambda_o d_a$ in (3) can be taken as constant, as the existing test data show little effect on the width of microcrack zone for the aggregate size usually used in construction. Equation (3) can therefore be expressed as follows:

$$\sigma_N = \left\{ B f_t' / [1 + (d/l_o)]^{1/2} \right\} + \alpha f_t'. \tag{4}$$

Jenq & Shah (1991) explained size-independent strength differently, based on the fracture behavior of concrete: the nominal strength σ_N was considered the sum of the size-independent and the size-dependent strengths, namely the former for the uncracked state and the latter for the cracked state, l_o being a characteristic length which can also be determined from regression analyses.

It can be seen from figure 2 that the size effect is insignificant for both very small and very large specimen sizes with the modified formula, as compared with the pronounced strength reduction, especially for very large sizes, with Bažant's formula. Furthermore, the size effect for transition sizes is apparent, but slightly decreased by the modified formula. This is because the ratio of the initial bond crack length to the specimen size gradually becomes smaller.

From the above discussion and the fact that cement-aggregate interfacial weakness can probably cause initial cracks through concrete, it is apparent that the size effect for concrete specimens with no initial artificially-made cracks occurs as a rather milder strength reduction than the severe one predicted by the previously derived size effect law. The validity of the above theoretical investigations was demonstrated by regression analyses on available test data for splitting tensile strength, shear strength, and uniaxial compressive strength (Kim *et al* 1989; Kim & Eo 1990).

3. Size effect on axial compressive strength

In the derivation of (1), the hypotheses include that total energy release is proportional to the area of the fracture process zone, $\lambda_o d_a a$ where λ_o is a constant and a is the length of crack band. However, it seems to be reasonable to assume that the fracture process zone width does not vary linearly with the maximum aggregate size d_a since cracks occur at a narrow strain-concentrated region. In other words, λ_o is a function of the maximum aggregate size rather than a constant. Therefore, the width of microcrack zone $\lambda_o d_a$ can be simply expressed as $\lambda_1 d_a^m$ (m = constant, $0 < m < 1$) even though it needs to be analysed more precisely by experiments or by theoretical means. The λ_1 may be, of course, a function of the strength of concrete since the microcrack zone for high-strength concrete is smaller than that of normal-strength concrete.

For the uniaxial compression strength, substituting for f_t' in (3) for the compressive strength of standard cylinder f_c', Kim & Eo (1990) and Kim *et al* (1989) proposed a model equation for prediction of compressive strength of cylindrical concrete specimens with height/diameter h/d of 2.0. Since the main crack in uniaxial compression usually occurs at stress of $0.7 \sim 0.85 f_t'$, size independent strength $\alpha f_c'$ can be taken as $0.7 \sim 0.85 f_c'$. However, tests by Smadi & Slate (1989) have shown that the value of α increases with increasing concrete strength. Thus, size independent strength $\alpha f_c'$ can be expressed as $\alpha(f_c') f_c'$. From the above discussion and the previous model equation (Kim *et al* 1989; Kim & Eo 1990) the nominal compressive strength of cylindrical specimens with h/d of 2.0 can be expressed as follows,

$$f_o = \left\{ B f_c' / \left[1 + (d/\lambda_1(f_c') d_a^m) \right]^{1/2} \right\} + \alpha(f_c') f_c', \tag{5}$$

where f_o is compressive strength of a cylindrical concrete specimen with diameter d.

3.1 *Derivation of modified size effect law for non-standard cylinder specimen*

Equation (5) can be applied to predict uniaxial compressive strength of cylindrical concrete specimens with h/d of 2.0. In order to apply for cylindrical specimens with different h/d, the

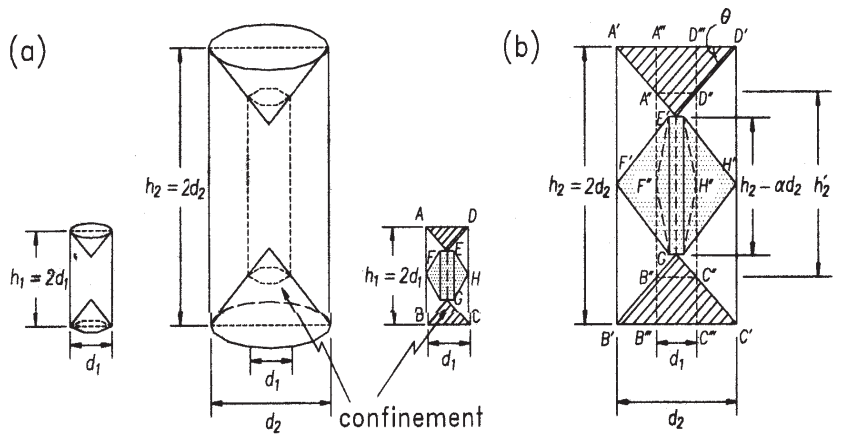

Figure 3. Characteristic length of general cylindrical specimens subjected to uniaxial compressive load.

equation should be modified to reflect the width of the microcrack zone and the characteristic dimension which provides the main crack zone.

When a cylindrical concrete specimen is subjected to uniaxial compression loads, it tends to expand in the lateral direction. However, there exists a frictional force between the machine platens and the specimen. This frictional force creates a lateral compressive force which is responsible for the formation of a cone at failure. When the lateral constraint is eliminated, the lateral compressive force disappears and a splitting type rupture is obtained. However, it seems to be valid to assume that the lateral constraint is produced to some extent since it is very difficult to eliminate the frictional force in practice.

In figure 3, when the frictional force is produced at failure, the characteristic dimension is represented by $(h_i - \beta d_i)$. It can be replaced by h_i or d_i especially when the specimens are geometrically similar since the ratios of the characteristic dimension $(h_1 - \beta d_1)/(h_2 - \beta d_2)$, h_1/h_2 and d_1/d_2 have the same value. But $(h_1 - \beta d_1)/(h_2 - \beta d_2)$ is not equal to h_1/h_2 if the specimens have the same diameter $(d_1 = d_2)$ as shown in figure 1b. In other words, the specimen which exhibits the size effect when the size is twice the size of the specimen denoted ABCD, is not the specimen denoted A‴B‴C‴D‴ which satisfies $h_2 = 2h_1$, but the specimen denoted A′B′C′D′ or the specimen denoted A″B″C″D″, which satisfies $(h_2 - \beta d_2) = 2(h_1 - \beta d_1)$ or $(h_2' - \beta d_1) = 2(h_1 - \beta d_1)$ respectively. This conclusion results from the condition that only the effects of the microcrack zone width and the characteristic dimension are considered to be factors influencing the size effect.

On the other hand, the size effect in uniaxial compressive strength is affected by the end restraints and energy release zone (denoted by dotted area in figure 3b, as well as the microcrack zone width and the characteristic dimension. Unless the confinement effect and the energy release zone are considered, the specimens A′B′C′D′ and A″B″C″D″ show the same size effect because this effect is only a function of the microcrack zone width and the characteristic dimension. The areas denoted A′E′D′ and A″E′D″ represent the confinement effects for specimens A′B′C′D′ and A″B″C″D″ respectively. Thus the specimen A′B′C′D′ has greater load resistant capacity than the specimen A″B″C″D″, as the confinement is related to the volume, i.e., $(d_2/d_1)^3$ while the stress is related to the area, i.e. $(d_2/d_1)^2$. But if the energy release zones are considered for the specimens, the specimen A′B′C′D′ has more energy per

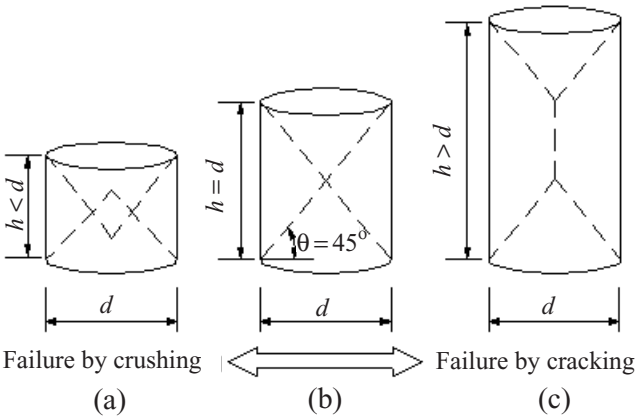

Figure 4. Failure modes with specimen geometry.

unit volume, that is, lower load resistant capacity per unit area (i.e. stress), than the specimen A″B″C″D″, since the same energy is required for the unit crack to be created. As a result, the effects of confinement and energy release zone on the size effect of uniaxial compressive strength are considered to be contradictory to each other. Furthermore, it is difficult to consider them for derivation of a size effect model as they have minor importance within a practical size range compared with the effects of microcrack zone width and the characteristic dimension. Consequently, (5) can be written as,

$$f_o = Bf_c'/\left[1 + (d/\lambda_1(f_c')d_a^m)(h/d - \beta)\right]^{1/2} + \alpha(f_c')f_c'. \tag{6}$$

It should be noted that the application of (6) is limited for cases $h \geq \beta d$ as shown in figure 4(b) and (c). If $h < \beta d$ as shown in figure 4a, the confinement zone extends through the specimen to lead failure by crushing, not by cracking. In this study, the value of θ shown in figure 3 was approximately selected as 45°.

3.2 *Considering the effects of maximum aggregate size and concrete strength*

From the statistical analyses of existing experimental data of Gonnerman (1925, 172 specimens), Blanks & McNamara (1935, 26 specimens), Department of the Interior (1965, 20 specimens), Kesler (1959, 337 specimens), and Murdock & Kesler (1957, 123 specimens) the empirical constants in (6) were determined. In this case, data numbers of specimens with $h/d = 2$ and $h/d \neq 2$ are 222 and 456 respectively, and the range of the maximum aggregate size is between 12.7 and 76.2 mm. From the regression analyses based on (6), it can be observed that the power of d_a is $m = 0.00055$. This means that since the value of $d_a^{0.00055}$ approaches 1.0, the effect of maximum aggregate size can be neglected within the practical range of size. It was shown that the effect of the concrete strength in (6) is also negligible.

3.3 *Without considering the effect of maximum aggregate size and concrete strength*

From statistical analyses, the following equation was derived for the same test results in the above section,

$$f_o = 0.4f_c'/[1 + (h - d)/50]^{1/2} + 0.8f_c', \tag{7}$$

where, f_o and f_c' are in MPa, and h and d are in mm. Figure 5 shows a comparison of the analytical and experimental values for plain concrete. The comparison indicates that

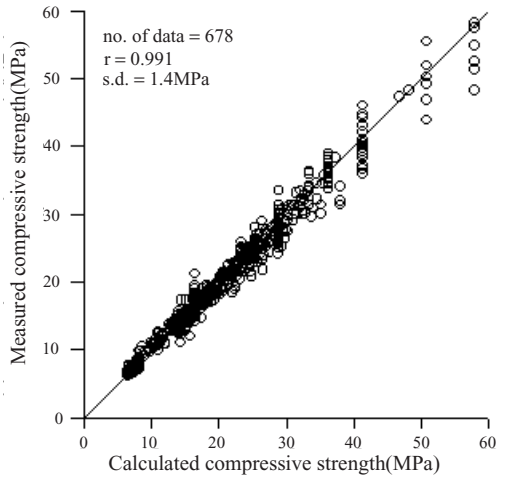

Figure 5. Comparison of analytical and experimental strength values of plain concrete cylinders.

the proposed equation gives a good prediction. Figure 6 shows the relationship between $1 + (h - d)/50$ and f_o/f_c' . From the same figure, it can be seen that most of the data are concentrated in a certain particular range since the diameters of most cylinders used in tests were 76,100, and 150 mm. When the value of h/d approaches 1.0, it is shown that the scatter of data is increased due to the effects of the confinement and energy release zone. Figure 6 also shows that the compressive strength of concrete would be 80% of the laboratory test results, since the confinement effects by frictional force would be negligible if the ratio, h/d, becomes very large.

4. Size effect on flexural compressive strength

In figure 7a, three different sizes of reinforced concrete beams are shown schematically. Reinforced concrete beams having different lengths with equal cross-sectional areas are shown in figure 7b. Reinforced concrete beams having the same lengths and thicknesses with different depths are shown in figure 7c. For over-reinforced concrete beams, the flexural strength

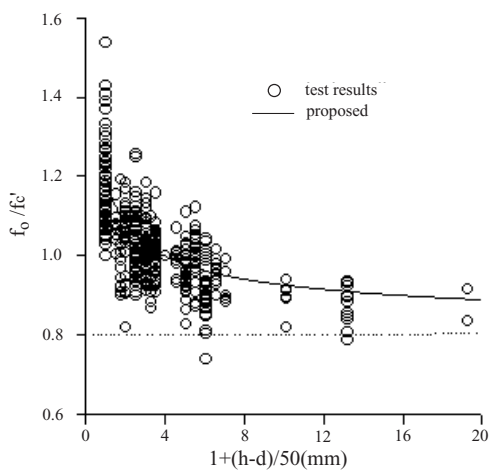

Figure 6. Relationship between $1+\{(h-d)/50\}$ and relative concrete strength (f_o/f_c').

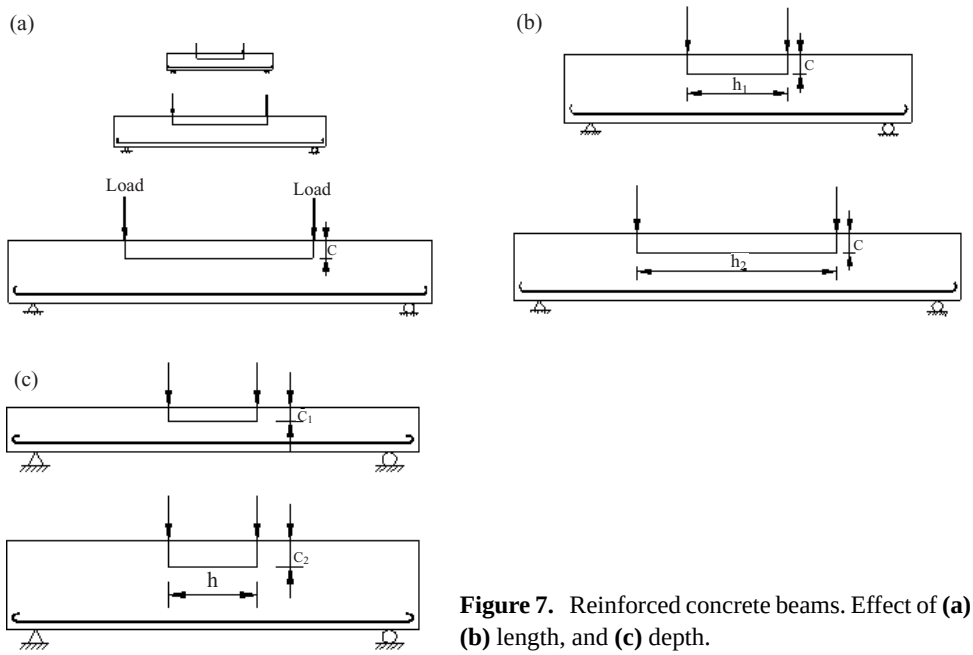

Figure 7. Reinforced concrete beams. Effect of **(a)** size, **(b)** length, and **(c)** depth.

is related directly to concrete strength between the two vertical loads and the neutral axis. However, in the case of under-reinforced beams the flexural strength is controlled mainly by the amount of tensile reinforcements. Therefore, the size effect of flexural strength for over-reinforced concrete beam is directly related to that of compressive strength in the compressive region. Also, the size effect of under-reinforced concrete beam is related to that of compressive strength, because the higher strength directly results in producing a longer moment arm.

For experiments on concrete beams (figure 7) subjected to flexural loads, the size, length, or depth effect cannot be evaluated systematically due to change in the location of the neutral axis of the cross section as member sizes, reinforcement ratios, applied loading increments, loading point locations etc. vary. To resolve these problems, a series of experiments for C-shaped concrete specimens (figure 8) subjected to axial load and bending moment are performed. The position of the neutral axis c is kept fixed by continuously monitoring strains on one surface of the C-shaped specimen and adjusting the eccentricity of the applied force so that the strain on the neutral surface remains zero.

4.1 *Main test variable*

The shape of specimens and the test procedures used are similar to those of Hognestad *et al* (1955), Kaar *et al* (1977), and Swartz (1985). The main test variable is a size ratio of 1:2:4 of the specimen to study the effect of size, where specimen depths are varied from 5 to 10 to 20 cm (figure 8a). The height h and width c are changed proportionally. Specimen length:depth ratios of 1:1, 2:1, 3:1, and 4:1 are used to study the effect of length, when constant depth ($c = 10$ cm) is maintained and specimen lengths are varied from 10 to 20 to 30 to 40 cm (figure 8b). Specimen length : depth ratios of 1:1, 2:1, and 4:1 are used to study the effect of depth when constant height ($h = 20$ cm) is maintained and specimen depths varied from 5 to 10 to 20 cm (figure 8c). The thicknesses of all specimens are kept constant ($b = 12.5$ cm)

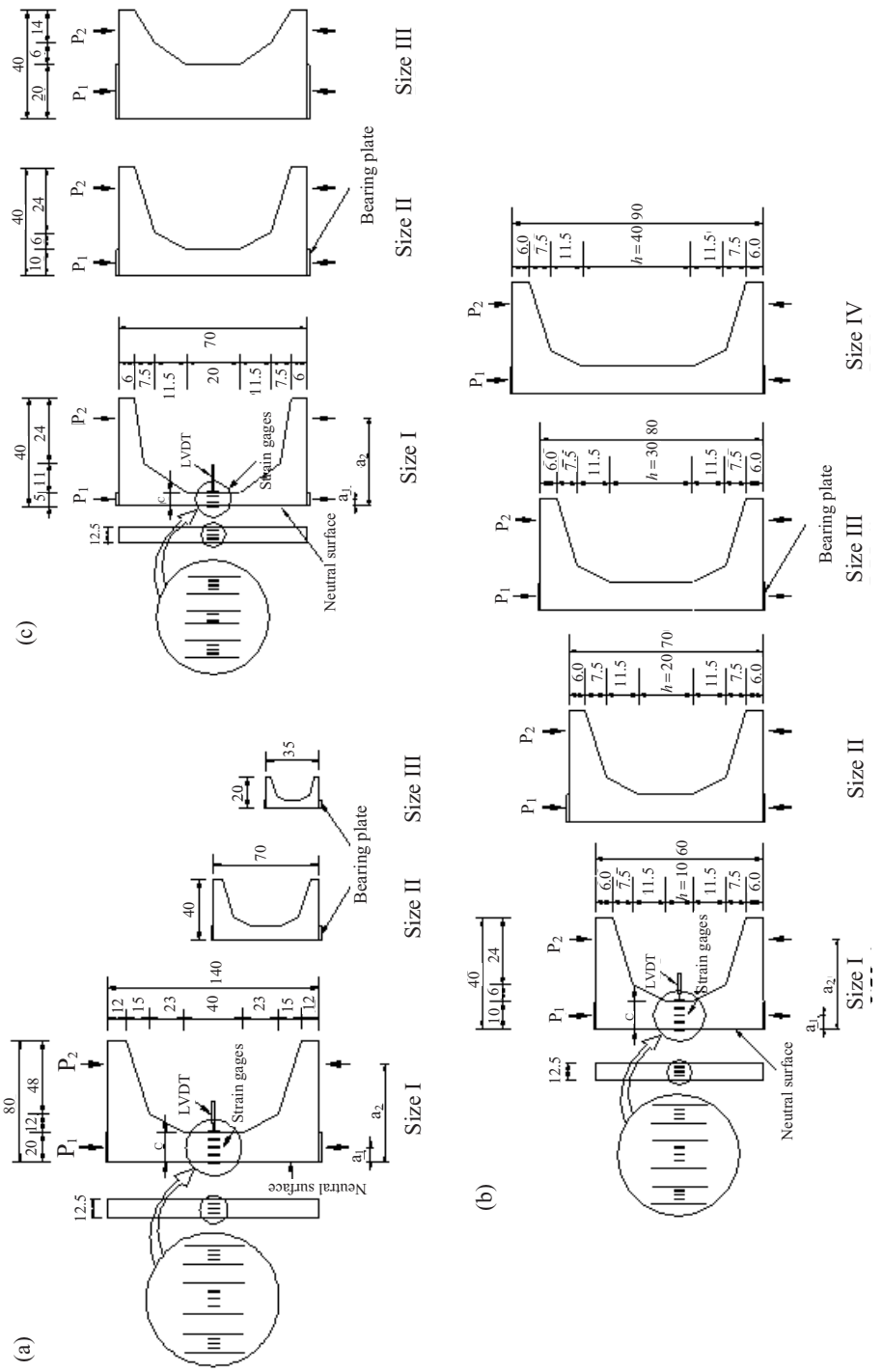

Figure 8. Size and shape of specimens (unit:cm). Effect of **(a)** size, **(b)** length and **(c)** depth.

Table 1. Concrete mix proportions.

		Unit weight (kg/m^3)				
w/c (%)	s/a (%)	W	C	S	G^*	SP^{**} (%)
37	40	178	480	676	1014	1

*Maximum aggregate size of 13mm; **super-plasticizer (ratio of cement weight)

to eliminate the out-of-plan size effect. The specimen thickness b is chosen to allow stable failure. The average concrete compressive strengths for the size, length and depth effect are 52, 58, and 55 MPa respectively.

4.2 *Mix design*

The concrete mix proportions selected for the C-shaped and 28-day compressive strength cylinder specimens are listed in table 1. Type I Portland cement is used. Maximum aggregate size d_a is 13 mm and superplasticizer and vibrator are used to improve workability and consolidation of concrete.

All beam specimens and test cylinders are removed from the mold after 24 h and wet-cured (specimens for size and length effect) and dry-cured (specimens for depth effect) in a curing room for 28 days until the testing date. Concrete compressive strength f_c', splitting tensile strength f_{ct}, and elastic modulus E_c are determined based on an averaged result of three identical $\phi 10 \times 20$ cm cylinders from the same batch. Table 2 tabulates the experimental data of f_c', f_{ct}, and E_c of the concrete cylinders where concrete from the same batch is used to cast C-shaped specimens for size, length, and depth effect tests. It is important to note that the tests on cylinder and C-shaped specimens for size, length, and depth effects are performed approximately 28 days after casting.

4.3 *Details of test specimens*

The dimensions, shape, and loading point locations of C-shaped specimens used in the experiments are shown in figure 8. The inner vertical thick solid lines of the hollow circle in figure 8 represent the locations where strain gauges are attached to the sides of specimens. More than three specimens per specimen size are prepared, because they are the minimum data points required for data curve fitting. The mid-height of C-shaped specimens which is the critical section under compression is not reinforced. Flexural and shear reinforcements are inserted at both ends of the specimen to eliminate undesired premature shear failure at the two end sections and ensure failure in the mid-height of the specimen. During testing, strains are measured up to failure at mid-height of specimen by twelve strain gauges. Two LVDTs are used to monitor the horizontal displacement at mid-height. This information is used to adjust the load lever arm distances a_1 and a_2 for calculation of bending moments.

Table 2. Physical properties of concrete.

	f_c' (MPa)	f_{ct} (MPa)	$E_c(\times 10^4)$ (MPa)
Size effect	52.0	5.0	3.10
Length effect	58.0	6.0	3.04
Depth effect	55.0	5.0	3.10

4.4 *Test procedure*

Displacement-controlled load application is used. Strain increments measured on the mid-height of specimen are 50×10^{-6} mm/mm for all sizes in the elastic region. However, near the peak stress and post-peak regions, strain increments are gradually reduced to ensure consistent failure in specimens of equal size. The major axial compressive load P_1, shown in figure 8, is applied using a universal testing machine (UTM) with a capacity of 2500 kN using a displacement control method. The minor load P_2, also shown in figure 8, is applied using a hand-operated hydraulic jack of 200 kN capacity.

The testing procedure is as follows:

(1) An increment of load P_1 is applied.
(2) P_1 is maintained while incrementally applying load P_2 and monitoring the strain value from the attached strain gauges on the tension face.
(3) On reaching zero strain value (on the average), the load P_2 is maintained while P_1 is further increased.
(4) This procedure is repeated until the specimen fails.

4.5 *Size effect of flexural compressive strength*

In order to obtain an analytical equation which can predict the flexural compressive strength of C-shaped specimens at failure, MSEL is used, and least squares method (LSM) regression analyses (IMSL Library; Benjamin & Cornell 1970) are carried out with 20 test data points. The width of the crack band l_o is empirically known to be related to maximum aggregate size, e.g., $l_o = \lambda_o d_a$ in which λ_o is approximately constant (2.0–3.0) (Bažant 1984; Kim *et al* 1999). In the regression analyses this constant was chosen as $2.0 \times d_a (= 2.6$ cm). Equation (8) is obtained from the analyses. The results are given in figure 9.

$$\sigma_N = \left[0.70 f_c' / (1 + (c/2.60))^{1/2}\right] + 0.47 f_c', \tag{8}$$

where nominal flexural compressive strength σ_N and uniaxial compressive strength f_c' are in MPa, and depth of C-shaped specimen c is in cm.

From the size effect law of Bažant and nonlinear regression analyses with the same data, (9) below is obtained,

$$\sigma_N = 0.96 f_c' / (1 + (c/22.27))^{1/2}. \tag{9}$$

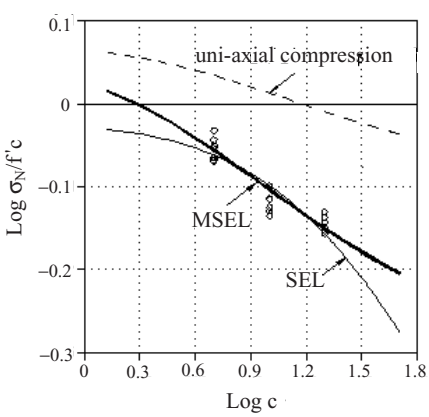

Figure 9. Comparisons of experiments with various equations.

Earlier (Kim *et al* 1999), proposed (7) to obtain the compressive strength of cylindrical concrete specimens with various diameters and h/d. For this purpose, the effects of the maximum aggregate size on the fracture process zone (FPZ) were considered and the concept of characteristic length was newly introduced.

Figure 9 shows the value σ_N/f_c' as a function of the depth c which is measured from the neutral axis to the compressive edge of the member. In this figure, the hollow circular data points, the thick solid line, the thin solid line, and the dashed line represent experimental data, and the results from (8), (9), and (7) respectively, as illustrated.

From figure 9, the results indicate a strong size effect condition. Especially, the new equation equation (8) shows best agreement with the experimental results. The reduction of flexural compressive strength at failure as the specimen size increases is stronger than that for uniaxial compressive strength. This is due to an FPZ for uniaxial compressive strength of cylinders is larger than that for flexural compressive strength of C-shaped specimens. Comparing (8) and (9), it can be seen that the size effect obtained from (8) is in better agreement with the experimental result than that from (9).

It is observed that for specimens having no initial crack or notch, use of the MSEL to predict their behaviour is appropriate.

4.6 *Size effect on ultimate strain (ε_{cu}) for flexural compression*

Since ultimate strain on the compressive outer layer of concrete beams subjected to flexural load is also affected by cracking, the size effect model for the ultimate strain can also be applied to the size effect law similar to that for stress (strength). In order to obtain a size effect equation that predicts the ultimate strain of C-shaped specimens at failure, LSM regression analyses are carried out, and (10) below is obtained. The relationship between $\varepsilon_{cu}/\varepsilon_{co}$ and $c/20$ is given in figure 10.

$$\varepsilon_{cu} = \left[1.70\varepsilon_{co}/\left(1 + 17(c/20)\right)^{1/2}\right] + 0.60\varepsilon_{co}, \tag{10}$$

where ε_{co} is the average ultimate strain for specimens with $c = 20.0$ cm.

In figure 10, the hollow circular data points, the thin solid line, and the thick dashed line represent experimental data and results from (8) and (10), respectively. This shows that ultimate strain decreases as the specimen size increases. The pattern is similar with flexural compressive strength. MSEL can be also used for the size effect of ultimate strain of C-shaped specimens.

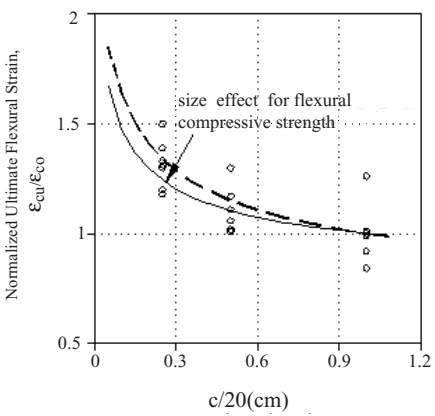

Figure 10. Comparison of ultimate strain with depth.

4.7 *Length and depth effect of flexural compressive strength*

Markeset (1995) and Markeset & Hillerborg (1995) experimentally showed that the post-peak energy per unit area is independent of the specimen length when the slenderness ratio is greater than approximately 2.50 for concrete cylinders. Jansen & Shah (1997) also experimentally showed that pre-peak energy per unit cross-sectional area increases proportionally with specimen length and post-peak energy per unit cross-sectional area does not change with specimen length for lengths greater than 20.0 cm in concrete cylinders. In this study, we conclude that flexural compressive strength does not change for specimens having a length greater than 30.0 cm for C-shaped reinforced concrete specimens as shown in figure 11.

The modified size effect equation proposed by Kim & Eo (1990) and Kim *et al* (1989) is used as the basic equation for the regression analyses of the experimental results of both length and depth size effect. The predicted depth size effect equation is given as

$$\sigma_N(c) = \left[Bf_c' / \left(1 + (c/l_o)\lambda(c)\right)^{1/2}\right] + \alpha f_c', \tag{11}$$

where the function $\lambda(c)$ represents the size of fracture process zone with a strain gradient and B and α are empirical constants of MSEL calculated as 0.70 and 0.47 (Kim *et al* 2000) respectively. In the regression analyses, l_o is chosen as 2.6 cm.

Due to the microcrack concentration at the failure zone which intensifies the strain gradient, the size effect becomes distinct. More specifically, if the value of c increases, then the strain gradient and size effect decrease. Therefore, it is assumed that the size of c is inversely proportional to the value of $\lambda(c)$. For the case of length-dependent size effect, the MSEL equation is similar to (11) except that the depth variable c is replaced by the length variable h where $\lambda(c)$ is then substituted with $\lambda'(h)$.

In order to obtain an analytical equation which predicts the flexural compressive strength of C-shaped specimens for length effect at failure, MSEL is used. LSM regression analyses are then performed on the results of 11 test data for length effect. Equation (12) is obtained as below from the analyses and the results are plotted as shown in figure 11.

$$\sigma_N(h) = \frac{0.70 f_c'}{\left\{1 + (h/2.6)\left(1.59\,(1/h)^{0.37}\right)\right\}^{1/2}} + 0.47 f_c', \ (h/c \le 3.0), \tag{12a}$$

$$\sigma_N(h) = 0.75 f_c', h/c \ge 3.0 \tag{12b}$$

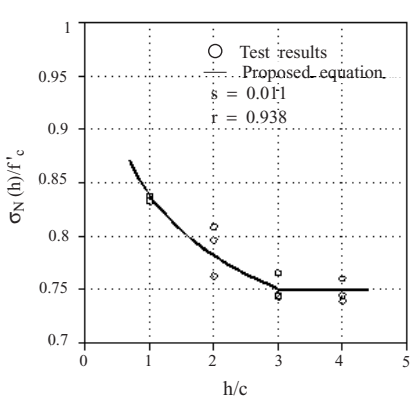

Figure 11. Normalized nominal strength with compressive strength versus ratio of length to depth.

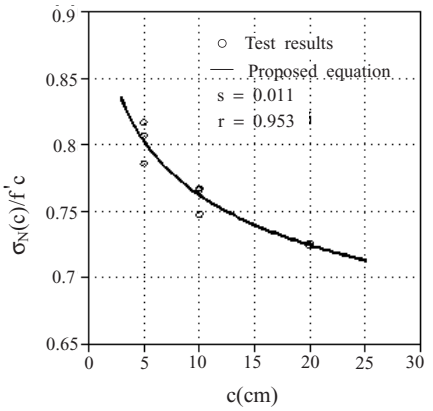

Figure 12. Normalized nominal strength with compressive strength versus depth.

where the length of the C-shaped specimen h is in centimetres. If the ratio of length to depth h/c is greater than or equal to 3.0, this ratio h/c is 3.0.

To develop an equation for depth effect, LSM regression analyses are also performed on the 8 results from the depth effect series. All techniques and notations are same as for length effect. Equation (13) is obtained from the analyses and the results are graphically shown in figure 12.

$$\sigma_N(c) = \frac{0.70 f_c'}{\left\{1 + (c/2.6)\left(4.17\,(1/c)^{0.53}\right)\right\}^{1/2}} + 0.47 f_c', \tag{13}$$

where depth of C-shaped specimen c is in centimetres. Figure 11 shows the value $\sigma_N(h)/f_c'$ as a function of the h/c, while figure 12 shows the value $\sigma_N(c)/f_c'$ as a function of the depth c . The hollow circular data points and the thick solid line in figures 11 and 12 represent experimental data and analytical results from (12) and (13) respectively. Figure 11 indicates strong length-dependent size effect. Equation (12) shows good agreement with the experimental results. For h/c greater than 3.0, the failure strength approaches a constant value of 0.75. Figure 12 shows a distinct depth dependent size effect when normalized with the compressive strength f_c' . Equation (13) shows reasonable agreement with the experimental results.

4.8 *Generalization of size effect law for C-shaped specimens*

Equation (14) below is obtained from LSM regression analyses of 39 experimental data,

$$\sigma_N(c, h) = \frac{0.70 f_c'}{\left\{1 + (c/2.6)\left(0.77\,(h/c)^{0.56} - 0.13\right)\right\}^{1/2}} + 0.47 f_c' \tag{14}$$

where if $h/c \geq 3.0$, h/c is 3.0, and notations are same as in (12) and (13). If the ratio h/c is 2.0, then the value of $\lambda(h/c)$ is 1.0 and (14) is the same as (8).

In figure 13, the thick solid line represents the analytical results obtained using (14) and the hollow circular data points represent the experimental data. The figure shows that (14) agrees quite well with the experimental results. Thus, flexural compressive strength of a beam specimen for various lengths and depths can be calculated by inputting c, h, and f_c' into (14).

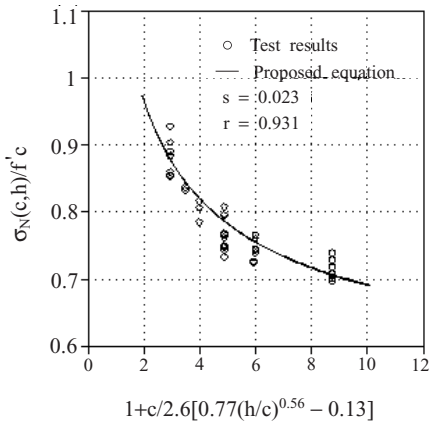

Figure 13. Normalized nominal strength with compressive strength as a function of $1 + \{c/2.6[0.77(h/c)^{0.56} - 0.13]\}$.

5. Conclusions

From studies for size effect on compressive strength of concrete, the following conclusions are drawn.

(1) Model equations for predicting the compressive strength of concrete cylinders are suggested based on nonlinear fracture mechanics. The effect of maximum aggregate size on the size effect of the compressive strength is negligible within the practical size range. This means that the effect of maximum aggregate size on the width of microcrack zone can be ignored compared with the effect of the characteristic dimension defined as $h_i - \beta d_i$.
(2) Size effect on flexural compressive strength is apparent, i.e., the flexural compressive strength at failure decreases as the specimen size increases. New parameter values of MSEL are suggested which better predict the "reduction phenomena" of the strength. Size effect for flexural compressive strength in C-shaped specimens is more distinct than that for uniaxial compressive strength of cylinders, and it can be expressed by the modified size effect law as well as that for ultimate flexural compressive strain.
(3) Length effect is apparent (i.e., the flexural compressive strength at failure decreases as the specimen length increases). Depth effect is also distinct. New parameter values of MSEL are suggested which better predict the "reduction phenomena" of the strength. More general parameter values are also suggested.
(4) The results suggest that the current strength criteria based design practice should be reviewed.

The authors would like to thank the Korea Institute of Science and Technology Evaluation and Planning (KISTEP) for financial support of the National Research Laboratory (NRL).

List of symbols

a length of crack band, crack length at failure;
a_o initial crack length;
b thickness of specimen;

B, α, β	empirical constants;
c	depth of C-shaped specimen;
d	characteristic dimension, diameter of cylinder;
d_1, d_2	diameters of cylinder;
d_a	maximum aggregate size;
E_c	elastic modulus of concrete;
f'_c	uniaxial compressive strength of standard concrete cylinder;
f_{ct}	splitting tensile strength of concrete cylinder;
f'_t	direct tensile strength of concrete cylinder;
f_o	compressive strength of general cylinder;
h	height of cylinder, length of C-shaped specimen;
h_1, h_2, h'_2	heights of cylinder;
l_o	width of crack band ($= \lambda_o d_a$);
m	constant, $0 < m < 1$;
P_1	major load;
P_2	minor load;
P_u	maximum load, or ultimate axial load $= P_1 + P_2$;
ε_{co}	average ultimate strain for specimen of $d = 20.0$ cm;
ε_{cu}	ultimate strain in concrete;
λ_o, λ_1	approximate constant ($= 2.0$);
$\lambda(c), \lambda'(h), \lambda(h/c)$	size of fracture process zone with a strain gradient;
θ	angle between surface of confined zone and plane perpendicular to cylinder axis;
σ_o	size independent stress ($= \alpha f'_t$);
σ_N	nominal flexural compressive strength at failure ($= P_u/bc$).

References

Bažant Z P 1984 Size effect in blunt fracture; concrete, rock, metal. *J. Eng. Mech., Am. Soc. Civil Eng.* 110: 518–535

Bažant Z P 1987 Fracture energy of heterogeneous material and similitude. *SEM-RILEM Int. Conf. on Fracture of Concrete and Rock* (Houston, TX: SEM-RILEM) pp 390–402

Bažant Z P 1989 Identification of strain-softening constitutive relation from uniaxial tests by series coupling model for localization. *Cement Concrete Res.* 19: 973–977

Bažant Z P 1993a Size effect in tensile and compressive quasibrittle failures. *JCI Int. Workshop on Size Effect in Concrete Structures* (Sendai: ICI) pp 141–160

Bažant Z P 1993b Size effect in tensile and compressive quasibrittle failure. *Proc. Int. Workshop, Size Effect in Concrete Structure*, Sendai, Japan (eds) H Mihashi, H Okamura, Z P Bažant (London: Chapman & Hall) pp 161–180

Bažant Z P, Chen E P 1997 Scaling of structural failure. *Appl. Mech. Rev., ASME* 50: 593–627

Bažant Z P, Xi Y 1991 Statistical size effect in quasi-brittle structures: II. Nonlocal theory. *J. Eng. Mech., Am. Soc. Civil Eng.* 117: 2623–2640

Bažant Z P, Xiang Y 1994 Compression failure of quasibrittle materials and size effect. *AMD Symp. Ser. ASME Appl. Mech. Div.*, 185, *Damage Mechanics in Composites, ASME Winter Annual Meeting*, Chicago (eds) D H Allen, J W Ju pp 143–148

Bažant Z P, Xiang Y 1997 Size effect in compression fracture: Splitting crack band propagation. *J. Eng. Mech., Am. Soc. Civil Eng.* 123: 162–172

Bažant Z P, Xi Y, Reid S G 1991 Statistical size effect in quasi-brittle structures: I. Is Weibull theory applicable? *J. Eng. Mech., Am. Soc. Civil Eng.* 117: 2609–2622

Benjamin J R, Cornell C A 1970 *Probability, statistics, and decision for civil engineers* (New York: McGraw-Hill) sec. 4.3

Blanks R F, McNamara C C 1935 Mass concrete tests in large cylinders. *ACI J. Proc.* 31: No. 280–303

Cotterell B 1972 Brittle fracture in compression. *Int. J. Fracture* 8: 195–208

Department of the Interior 1965 Mass Concrete Investigations Bulletin No. 4, Final Report, Boulder Canyon Project-Part VII, Cement and Concrete Investigations, US Bureau of Reclamation

Gonnerman H F 1925 Effect of size and shape of test specimen on compressive strength of concrete. *Proc. ASTM.* 25: 237–250

Hillerborg A 1988 Fracture mechanics concepts applied to moment capacity and rotational capacity of reinforced beams. *Proc. Int. Conf. Fracture and Damage Mechanics of Concrete and Rock*, Vienna, pp 233–240

Hognestad E, Hanson N W, McHenry D 1955 Concrete stress distribution in ultimate strength design. *ACI J. Proc.* 52: 455-479, also PCA Deve. Bull. D6

IMSL Library, Edition 8, IMSL, Inc.

Jansen D C, Shah S P 1997 Effect of length on compressive strain softening of concrete. *J. Eng. Mech., Am. Soc. Civil Eng.* 123: 25–35

Jenq Y S, Shah S P 1991 Features of mechanics of quasi-brittle crack propagation in concrete. *Int. J. Fracture* 51: 103–120

Kaar P H, Hanson N W, Capell H T 1977 Stress-strain characteristics of high-strength concrete PCA Research and Development Bulletin RD051.01D, pp 1–10

Kesler C E 1959 Effect of length to diameter ratio on compressive strength–An ASTM cooperative investigation. *Proc. ASTM* 59: 1216–1229

Kim J K, Eo S H 1990 Size effect in concrete specimens with dissimilar initial cracks. *Maga. Concrete Res.* 42: 233–238

Kim J K, Eo S H, Park H K 1989 Size effect in concrete structures without initial crack. *Fracture mechanics: Application to concrete* (Detroit: ACI) SP-118, pp 179–196

Kim J K, Yi S T, Park C K, Eo S H 1999 Size effect on compressive strength of plain and spirally reinforced concrete cylinders. *ACI Struct. J.* 96: 88–94

Kim J K, Yi S T, Yang E I 2000 Size effect on flexural compressive strength of concrete specimens. *ACI Struct. J.* 97: 291–296

Kim J K, Yi S T, Kim J H J 2001 Effect of specimen sizes on flexural compressive strength of concrete. *ACI Struct. J.* 98: 416–424

Markeset G 1995 A compressive softening model for concrete. *Fracture mechanics of concrete structures* (ed.) F H Wittmann (FRAMCOS-2, AEDIFICATIO Publishers) pp 435–443

Markeset G, Hillerborg A 1995 Softening of concrete in compression localization and size effects. *Cement Concrete Res.* 25: 702–708

Murdock J W, Kesler C E 1957 Effect of length to diameter ratio of specimen on the apparent compressive strength of concrete. *ASTM Bull.* (221) 68–73

Rokugo K, Koyanagi W 1992 Role of compressive fracture energy of concrete on the failure behaviour of reinforced concrete beams. *In Applications of Fracture mechanics to reinforced concrete* (ed.) A Carpenteri (Elsevier Applied Science) pp 437–464

Smadi M M, Slate F O 1989 Microcracking of high and normal strength concretes under short- and long-term loadings. *ACI Mater. J.* 86: 117–127

Swartz S E, Nikaeen A, Narayan Babu H D Periyakaruppan N, Refai T M E 1985 Structural bending properties of higher strength concrete. *High-Strength Concrete* SP-87: 147–178

Van Mier J G M 1992 Scaling in tensile and compressive fracture of concrete. In *Applications of fracture mechanics to reinforced concrete* (ed.) A Carpenteri (Elsevier Applied Science) pp 95–135

Vonk R A 1992 *Softening of concrete loaded in compression*. Ph D thesis, Eindhoven University of Technology, Eindhoven